Korean J. Chem. Eng., **24**(2), 197-203 (2007)

Heat transfer behavior of high-power light-emitting diode packages

Hyun-Wook Ra, Kwang Sup Song*, Chi-Won Ok and Yoon-Bong Hahn†

School of Chemical Engineering and Technology, Chonbuk National University, Jeonju 561-756, Korea
* Korea Institute of Energy Research, Daejeon 305-343, Korea
(*Received 7 June 2006 • accepted 9 October 2006*)

Abstract–Heat transfer characteristics of a high-power light-emitting diode (HPLED) have been carried out in terms of experiment and simulation. Finite volume method was used to analyze the temperature and thermal stress distributions in the HPLED package as a function of drive current and package structure. Predicted temperatures of silicone encapsulant and epoxy resin showed a good agreement with measured temperatures. The thermal stress increased with the drive current due to a heat burden. The intersection edges between the light emitting diode chip and the silicone encapsulant showed a higher thermal stress. The thermal stress of Cu-thin-film coated package was lower than that of other package structures because of an efficient cooling effect.

Key words: Light-emitting Diode, Junction Temperature, Heat Transfer, Thermal Management

INTRODUCTION

Light emitting diodes (LEDs) conventionally have been used for indicators. The brightness and durability of the LEDs and laser diodes (LDs) make them ideal for display, optical communications, optical storage, etc. Recently, the introduction of high-brightness LEDs with white light and monochromatic colors has led to movement towards specialty and general illumination applications. The high-brightness LEDs are expected to replace incandescent and fluorescent lamps in the near future because of much less consumption of energy. The increased electrical currents used to drive the LEDs have focused more attention on thermal management because the efficiency and reliability of LEDs strongly depend on successful thermal management [1,2].

Most of the power applied to the LED is dissipated as heat, depending on the power dissipation and the resistance to heat-flow. Thus the internal temperature of the LED is determined not only by the ambient temperature, but also by the drive current and thermal resistance. Due to a difference in coefficients of thermal expansion, the LED package is under thermal stress when it is exposed to high internal temperatures beyond a maximum rating or repeated thermal cycles. Such a thermal stress thus induces cracking, delamination, or broken bond wires, which can cause catastrophic failures. Therefore, an effective removal of heat to maintain a safe junction temperature is the key to meeting the future flux per LED requirements [3-5]. The thermal properties of the LED package are also dependent on the shape of heat slug through which the heat is transported to the ambient atmosphere. A typical is a cylindrical-shaped heat slug.

In this work, to analyze the temperature and thermal stress in a high-power LED (HPLED) package, the finite volume method (FVM) was used as a function of drive current and package structure for a thermal design. A typical dome-shaped HPLED package was adopted for simulation and four different geometrical structures were examined for the shape of heat slug. The CFD-ACE+ code was used for simulation. To verify the numerical model, the junction temperature of the LED and the temperature inside the HPLED package were measured and compared with predicted results.

†To whom correspondence should be addressed.
E-mail: ybhahn@chonbuk.ac.kr

MATHEMATICAL MODEL

1. Description of High Power LED Package

Fig. 1 shows a schematic cross section of an HPLED package. The LED chip was grown by metal organic chemical vapor deposition on sapphire substrates. The LED active region consists of multiple quantum wells consisting of $In_xGa_{1-x}N$ wells and GaN barriers [6-8]. The length of the chip was approximately 1 mm and the

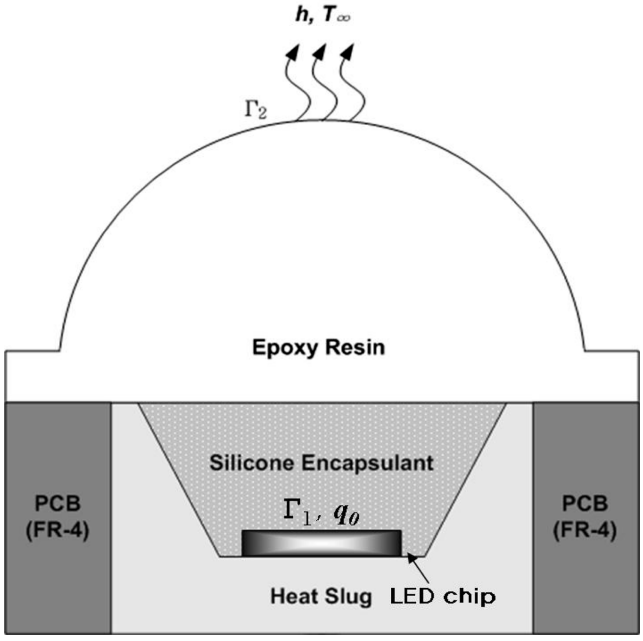

Fig. 1. Cross section view of high-power LED package and boundary conditions.

thickness around 150 μm, attached with a conical-type Cu heat slug. The conical angle at the walls is vital to obtain the most effective light extraction from the chip package. The conical angle walls create some space, which is filled with a phosphor/silicone mixture encapsulant. A clear epoxy resin is molded over the silicone encapsulant to form a lens which protects and guides the light from the devices. Heat transfer from the LED chip is through the exposed surface by the conduction and by the natural convection to the ambient.

2. Heat Transfer

The governing equation for the heat-transfer analysis of the HPLED package is given by

$$k\nabla^2 T + Q = \rho C \frac{\partial T}{\partial t} \tag{1}$$

where k, Q and C represent thermal conductivity, rate of heat generation and specific heat, respectively.

Two types of boundary condition are needed to solve Eq. (1), as presented in Fig. 1:

$$q_i n_i = -q_0 \quad \text{at} \quad \Gamma_1 \tag{2}$$

$$q_c = h(T_b - T_\infty) \quad \text{at} \quad \Gamma_2 \tag{3}$$

where q_i is the heat flux toward all directions, n_i is the normal vector, q_0 is the heat flux generated from the LED chip, q_c is the net heat flux at the boundary, h is the convective heat transfer coefficient, T_∞ is the ambient temperature, T_b is the temperature at the boundary, and Γ_1 and Γ_2 represent the chip and package boundaries, respectively [9,10].

Eqs. (2) and (3) can be rearranged in a general form of boundary condition as follows

$$q_i n_i = -MT_b + S \quad \begin{cases} M = h,\ S = hT_\infty \text{ for Convection} \\ M = 0,\ S = \pm q_0 \text{ for Conduction} \end{cases} \tag{4}$$

3. Thermal Stress

Thermal stress in a material is caused by the difference in coefficient of thermal expansion (CTE). In this case, the estimation of thermal stress developed in the electronic cooling can be expressed as

$$\sigma(T) = \int_T^{T_J} \frac{\alpha - \alpha_T}{\frac{1}{E(T)} + \frac{A}{E}} dT \tag{5}$$

where σ is the induced thermal stress, T_J is the junction temperature, E is Young's modulus, A is geometric factor with the order of unity, α and E(T) are the CTE and the storage modulus, respectively.

Table 1. Properties of the materials used for high-power LED package simulation

Materials	Thermal conductivity ($W m^{-1} K^{-1}$)	Young's modulus (GPa)	CTE (ppm/°C)	Poisson's ratio
Epoxy resin	0.19	3.45	69	0.37
Heat slug (Cu)	395	118	16.6	0.34
FR-4 (PCB)	0.17	24	15	0.0136
Silicone encapsulant	0.15	2.8	80	0.055
Thermal paste	1.1	0.2	2.76	0.028

At $T < T_g$ (glass transient temperature), α is nearly independent of temperature. Since the E is much larger than E(T), Eq. (5) can be simplified as

$$\sigma(T) = \int_T^{T_J} (\alpha - \alpha_T) E(T)\ dT \tag{6}$$

The properties of the materials used in the LED package are summarized in Table 1 and assumed to be independent of the temperature because the temperature rise in the package is not high enough to change the properties [11,12].

MEASUREMENTS OF JUNCTION AND PACKAGE TEMPERATURES

Junction temperature (T_J) of the LED chip affects the performance of an HPLED because the light-output center wavelength, power magnitude, and reliability are all directly dependent on the junction temperature. Thus, the effective management of the heat evolved from the LED chip is crucial to the overall performance of the HPLED. Validation of thermal management requires the ability to measure the junction temperature. Several methods have been reported to determine the LED junction temperatures, for instance, infrared imaging method [13], liquid crystal thermography [14], and use of LED light-output [15]. In this work, LED's electrical characteristics were used to measure the junction temperature of the HPLEDs [16]. It has been reported that at a given forward current, the forward voltage across the LED decreases linearly with an increase in temperature. Therefore, by comparing the LED voltage to a reference condition, the junction temperature can be determined. The junction temperature can be expressed as

$$T_J = T_A + \frac{V_t - V_A}{K} \tag{7}$$

where T_A is the reference ambient temperature, V_t and V_A are the forward voltages at the test condition and the reference ambient temperatures, respectively, while K is the temperature coefficient of the forward voltage.

Eq. (7) can be rearranged to obtain an expression for K, which is called the K factor:

$$K = \frac{V_0 - V_1}{T_0 - T_1} \tag{8}$$

where V_0 and V_1 are forward voltages at two known ambient temperature of T_0 and T_1, respectively. Therefore, the constant K can be determined by measuring the voltage drop across the LED junction at the two known ambient temperatures. The junction temperature of the LED can be determined by using Eq. (1) with measuring the change in the forward voltage.

To implement this method of measuring the junction temperature, an electronic circuit was built to power the LED and to measure the voltage across the junction. Fig. 2 shows a schematic illustration of the experimental setup which consists of three parts: the thermal chamber, the heating system, and the drive circuit. The LED was placed inside the thermal chamber at 25 °C and was driven at four different current conditions of 150, 200, 250, and 300 mA. The LED was connected to a power supply and a digital multimeter out-

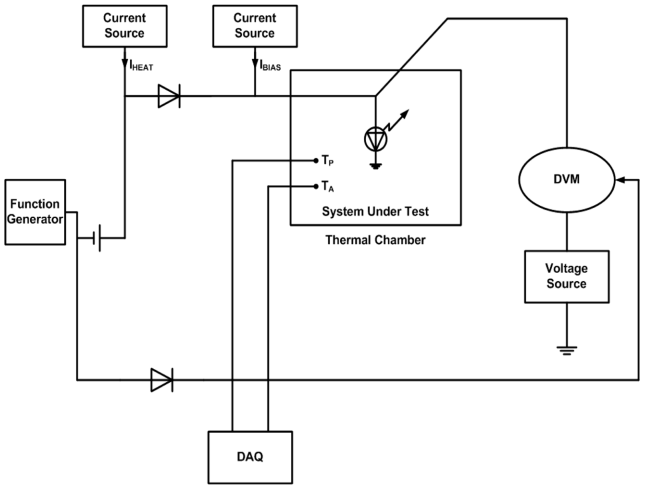

(a) Junction temperature measurement system

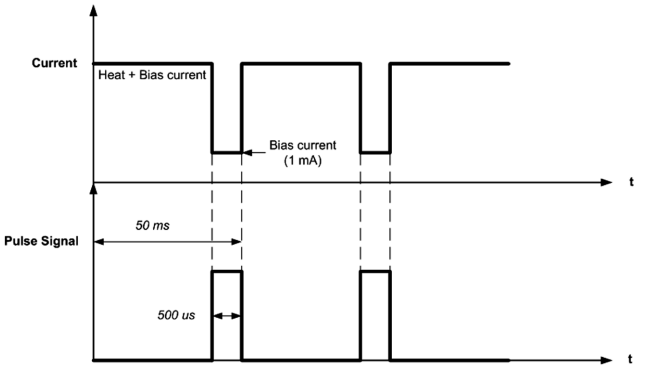

(b) Sequence of applied currents

Fig. 2. Schematic diagram for measuring the LED junction temperature.

side the chamber by routing the wires through a small hole. A heating element was placed at the bottom of the chamber. A resistance temperature detector (RTD) measured the ambient temperature of the chamber and provided a feedback signal to maintain the temperature inside the chamber within error range of ±1 °C. A J-type thermocouple was used to monitor the junction temperature of the LED. The temperature data from the thermocouple was used in parallel with the temperature obtained from the RTD to determine thermal equilibrium. At regular intervals the current was stepped down to a value of 1 mA by using a very short square-wave pulse (500 μs). The voltage across the junction was measured during this short-stepped-down period. It was assumed that the 1 mA current provides negligible heat to the junction ((b), Fig. 2). In addition, during the short-stepped-down pulse condition, the temperature drop was also negligible. The LED drive circuit provided the necessary current to the LED while the oscilloscope monitored the drive current and voltage across the LED.

At each experimental condition, the measured voltage across the junction determined the junction temperature. Fig. 3 shows that the junction temperature of the HPLED is linearly proportional to the drive current. Therefore, it can be concluded that heat at the junction increases with increasing the drive current. In other words, an

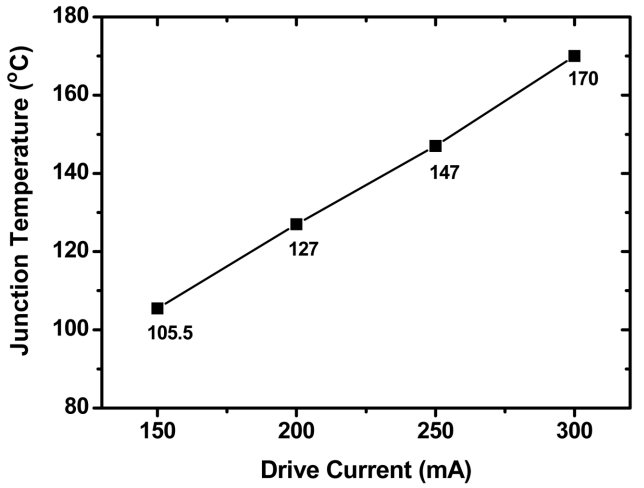

Fig. 3. Junction temperature of high-power LED as a function of drive current.

increment in junction temperature leads to a gain in the drive current.

The temperatures of the HPLED package were also measured and compared with the numerical results. The temperature profile inside the HPLED package was measured with a micro-thermocouple embedded into the package. Fig. 4 schematically shows the system for temperature measurement of HPLED package, in which the temperatures of silicone encapsulant and epoxy resin were measured by the micro-thermocouple for the HPLED package placed in a constant-temperature oven.

RESULTS AND DISCUSSION

The effect of drive current on the temperature distribution of the HPLED package is shown in Fig. 5. The temperature of the HPLED package increases with drive current. This is explained by the fact that heat generation at the junction increased with the drive current. Particularly, silicone encapsulant and epoxy resin show a higher temperature due to heat accumulation. The higher temperatures of silicone encapsulant and epoxy resin induce problems such as bonding-wire breakage. When the temperatures of silicone encapsulant and epoxy resin are greater than the glass transition temperature, the CTE increases about three times. If the HPLED is thermally cycled above the glass transition temperature, the Au-bonding wire gets thermal stress and breaks down. The predicted temperatures are compared with measured data in Fig. 6. The numerical predictions showed a good agreement within about 5% error.

Fig. 7 shows the effect of drive current on the thermal stress distribution of the high power LED package. The thermal stress of high power LED package increases with the drive current, especially at the intersection edges between the LED chip and silicone encapsulant. Excessive thermal stress can cause delamination between the LED chip and the encapsulant, which forms a thin chip-air-silicone interface inside the package. Although this problem does not generally induce a catastrophic failure, it can result in permanent reduction in light output. The delamination can either occur between the phosphor coating and the silicone encapsulant or between the LED chip and the phosphor coating. Therefore, thermal management is very important for reliability of the high power LED.

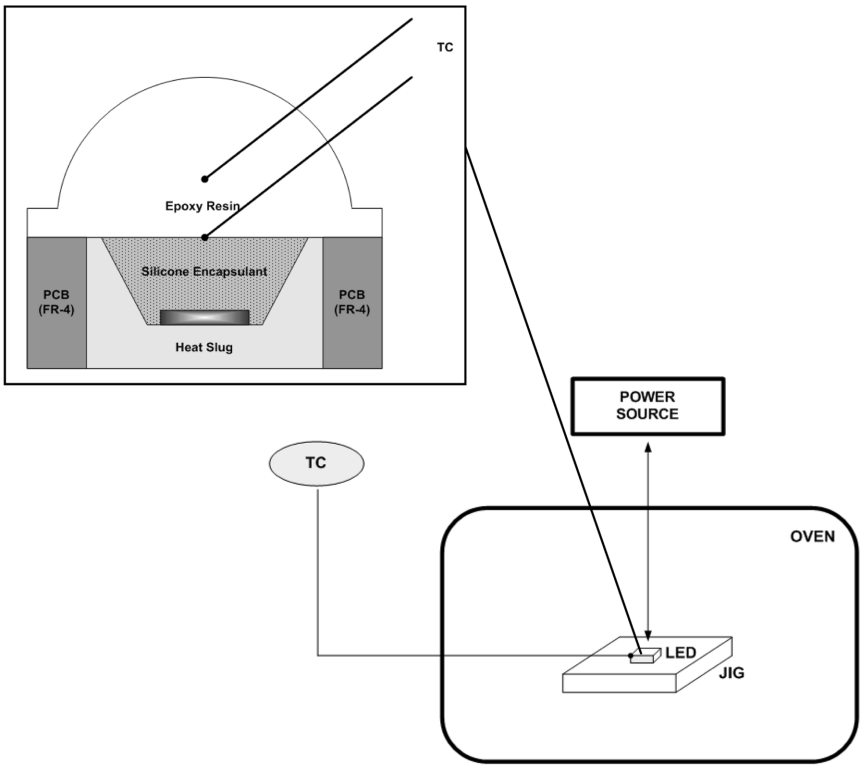

Fig. 4. Systematic illustration of the system used for temperature measurements inside high-power LED.

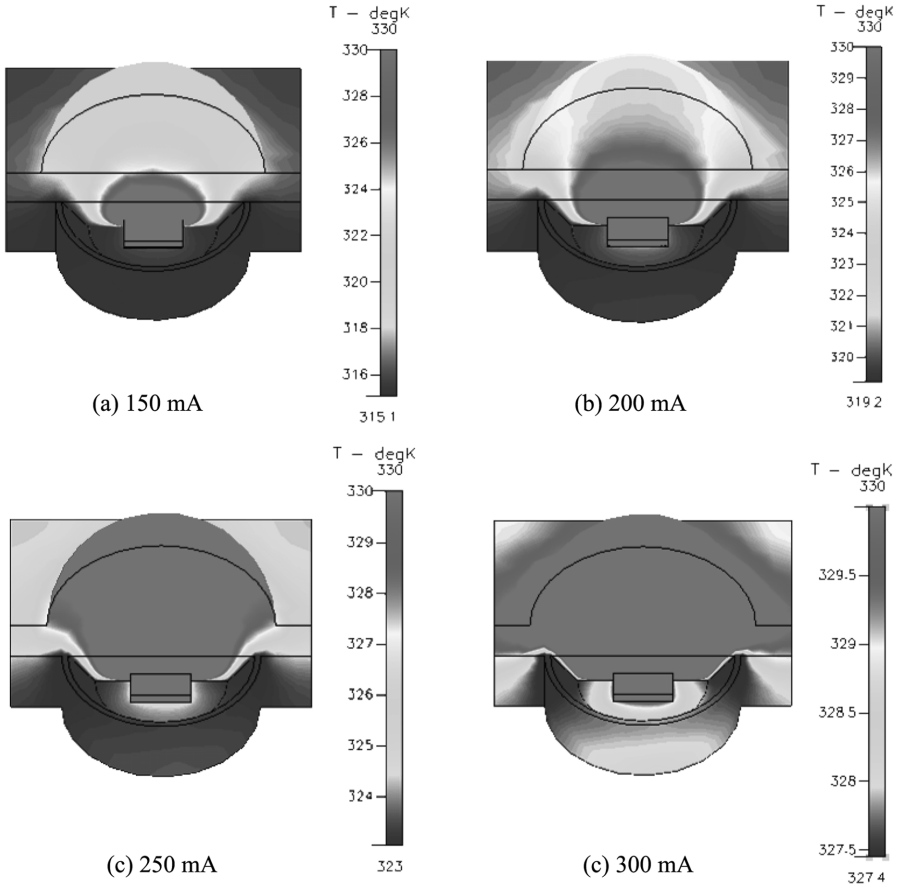

Fig. 5. Temperature distributions of high-power LED package as a function of drive current.

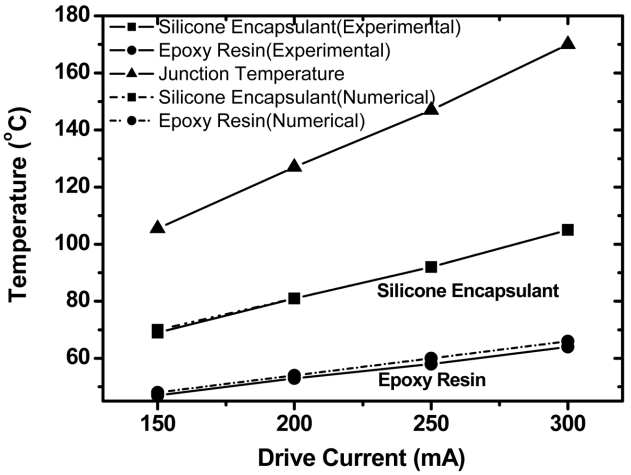

Fig. 6. Comparison between measured and predicted temperatures of silicone encapsulant and epoxy resin as a function of drive current.

Structural geometry of the HPLED package also has an influence on the thermal properties. Most heat from the LED package may be transported through the heat slug by conduction and finally to the ambient by convection. Fig. 8 demonstrates various kinds of package structures: (a) a cylindrical-shaped heat slug which has an expanded volume, (b) a cone-shaped heat slug with increased area, (c) a hexahedron-shaped heat slug, and (d) a 20 μm Cu-thin-film coated package on a printed circuit board (PCB).

Fig. 9 reveals the temperature distributions with various package structures, predicted at 300 mA drive current. The cylindrical-shaped heat slug (a), having expanded volume, shows a low temperature distribution inside the package due to more heat dissipation between the heat slug and the ambient by convection. A similar result was obtained in the case of hexahedron-shaped heat slug (c), i.e., a relatively low temperature distribution inside the package. The cone-shaped heat slug (b) shows an increase of heat burden around the tip of the cone. However, efficient heat dissipation was observed with the cu-coated package on PCB (d). This efficient heat dissipation is attributed to more heat removed to the ambient through the conductive Cu film by combined conduction and convection mechanisms.

Fig. 10 shows the thermal stress distributions of the package structures, predicted at 300 mA drive current. The cylindrical-shaped heat slug (a) shows a low thermal stress inside the package. The thermal stress of the hexahedron-shaped heat slug (b) is relatively higher than that of other structures. This is explained by the fact that stress was accumulated at the tip of the heat slug. However, the Cu-coated package on PCB (c) shows the lowest thermal stress distribution due to the efficient heat dissipation.

SUMMARY AND CONCLUSIONS

To analyze thermal properties of a high power LED package for reliability improvement, the junction temperature of the high power LED was measured by using the LED's electrical characteristics. Based on the measured junction temperature, the FVM was used to analyze the temperature and thermal stress distribution in the high power LED package as a function of drive current and package structure. The junction temperature of the LED increased with the drive current and thus increased the package temperature and thermal stress itself. Silicone encapsulant and epoxy resin showed a higher temperature distribution. The thermal stress in the package was in-

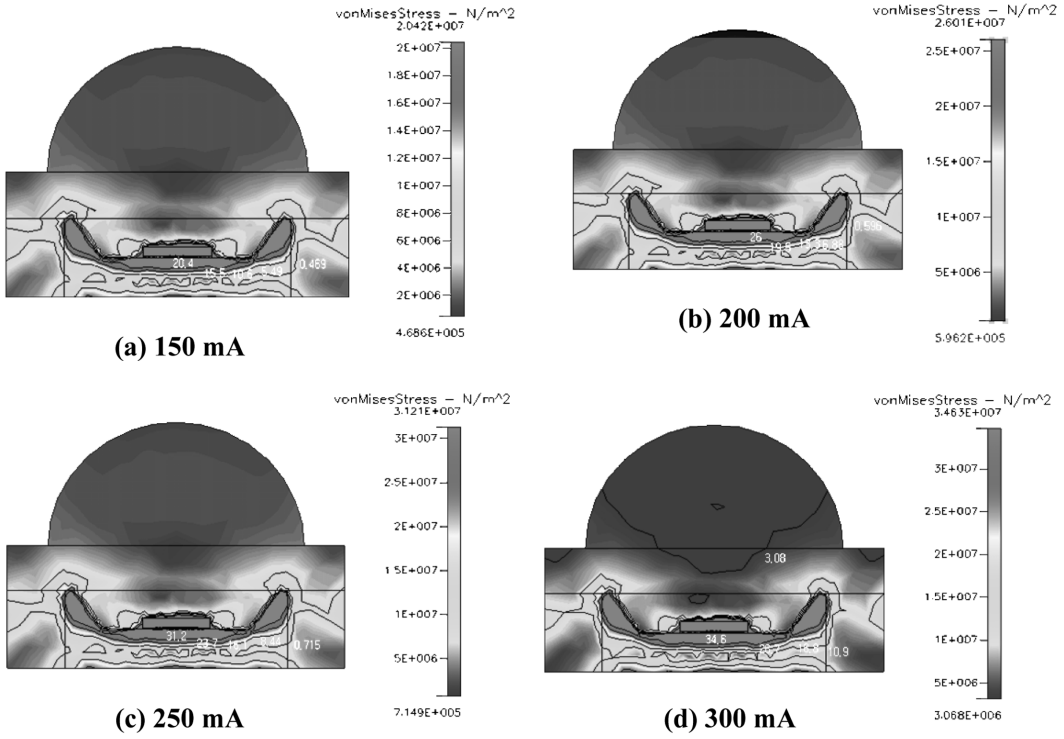

Fig. 7. Thermal stress distributions of high-power LED package as a function of drive current.

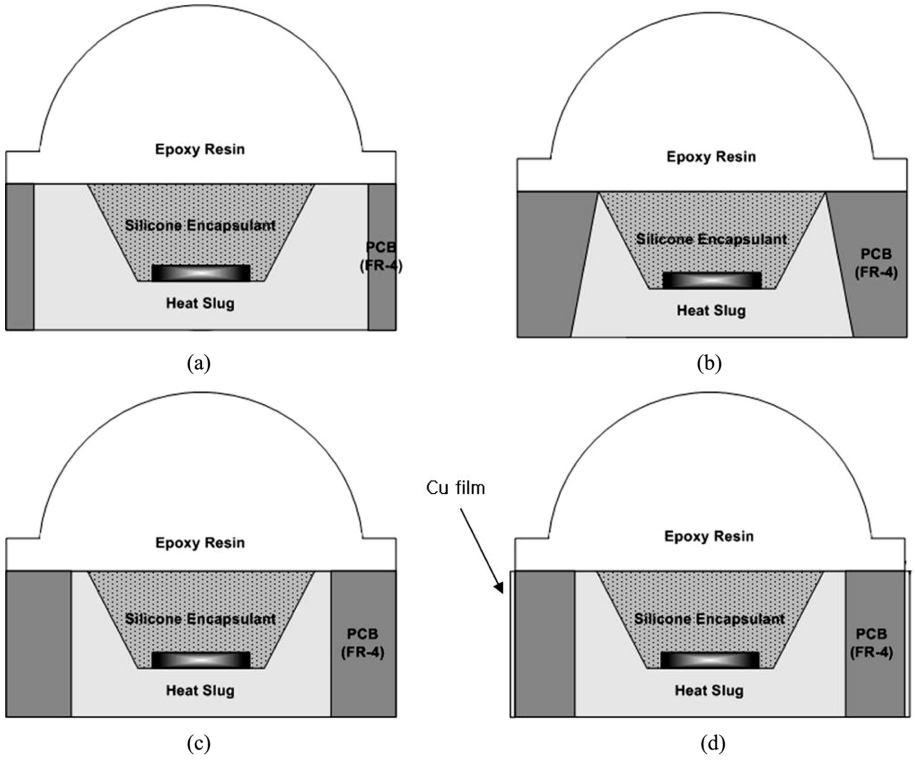

Fig. 8. Various package structures of high-power LED: (a) cylindrical-shape, (b) cone-shape, (c) hexahedron-shape, and (d) Cu-thin-film coated package.

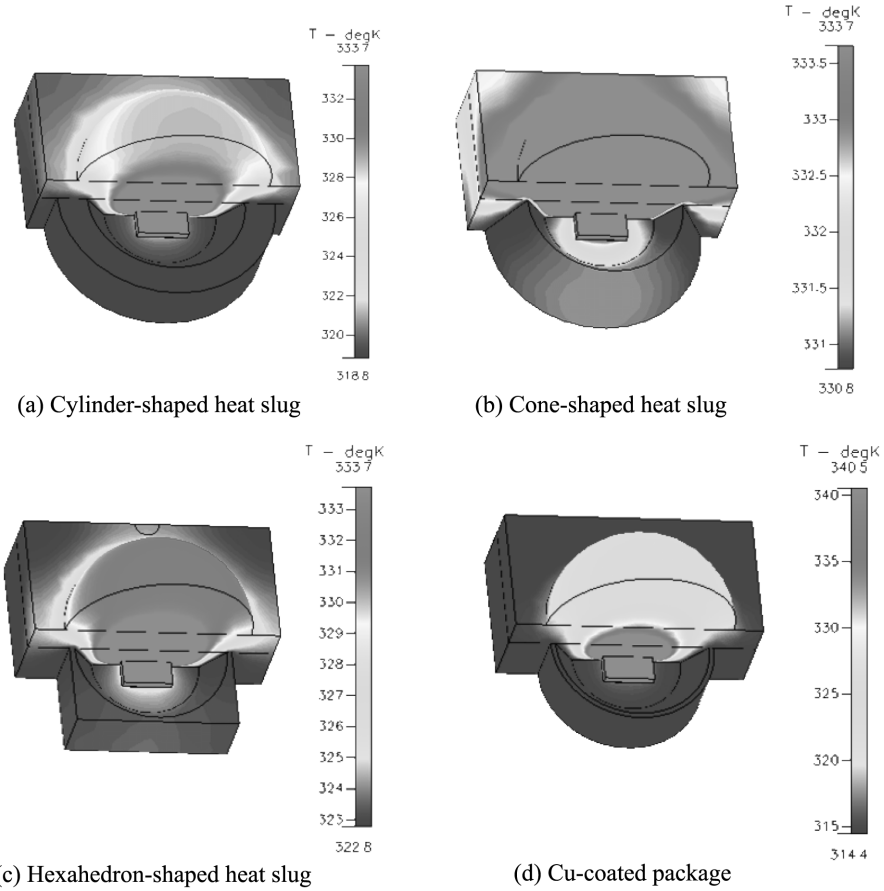

Fig. 9. Temperature distributions of high-power LED package with various package structures at 300 mA drive current.

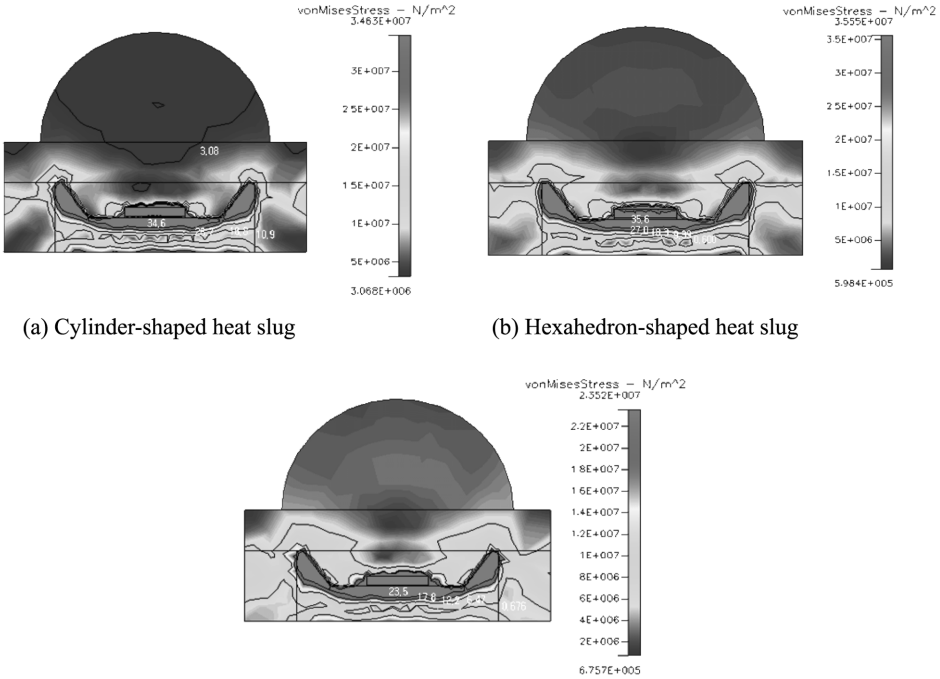

(a) Cylinder-shaped heat slug (b) Hexahedron-shaped heat slug

(c) Cu-coated package

Fig. 10. Thermal stress distributions of the high-power LED package with various package structures at 300 mA drive current.

creased at intersection edges between LED chip and silicone encapsulant due to heat burden. Increasing the area and volume of the heat slug resulted in more efficient cooling. Especially, the Cu-thin-film coated package showed the best heat dissipation and lower thermal stress distribution than that of other package structures.

ACKNOWLEDGMENTS

This paper was supported in part by the Korea Research Foundation (KRF-2005-005-J07502) funded by Korea government (MOE-HRD) and by the NRL program through the Korea Institute of Energy Research (KIER).

REREFENCES

1. R. V. Steele, *Proc. of SPIE*, **4445**, 1 (2001).
2. F. M. Steranka, J. Bhat, D. Collins, L. Cook, M. G. Craford, R. Fletcher, N. Gardner, P. Grillot, W. Goetz, M. Keuper, R. Khare, A. Kim, M. Krames, G. Harbers, M. Ludowise, P. S. Martin, M. Misra, G. Mueller, R. Mueller-Mach, S. Rudaz, Y.-C. Shen, D. Steigerwald, S. Stockman, S. Subramanya, T. Trottier and J. J. Wierer, *Phys. Stat. Sol. (a)*, **194**(2), 380 (2002).
3. M. Arik, J. Petroski and S. Weaver, *Proc. of the ASME/IEEE ITHERM-Conference*, San Diego (2002).
4. N. Narendran, J. D. Bullough, N. Maliyagoda and A. Bierman, *J. Illum. Eng. Soc.*, **30**(1), 57 (2002).
5. LUMILEDS, *Application Brief*, **AB25** (2004).
6. R. J. Choi, Y. B. Hahn, H. W. Shim, E.-K. Suh, C.-H. Hong and H. J. Lee, *Korean J. Chem. Eng.*, **20**, 1134 (2003).
7. R. J. Choi, H. J. Lee, Y. B. Hahn and H. K. Cho, *Korean J. Chem. Eng.*, **21**, 292 (2004).
8. R. J. Choi, E.-K. Suh, H. J. Lee and Y. B. Hahn, *Korean J. Chem. Eng.*, **22**, 298 (2005).
9. T. J. Lu, *Int. J. of Heat and Mass Transfer*, **43**, 2245 (2000).
10. J. H. Lienhard IV and V. J. H. Lienhard, *Heat transfer textbook*, 3rd ed., Phlogiston Press, Massachusetts (2004).
11. R. J. Hannemann, A. D. Kraus and M. Pecht, *Semiconductor packaging: A multidisciplinary approach*, 1st ed., John Willey & Sons, New York (1994).
12. C. A. Harper, *Electronic materials and processes handbook*, 3rd ed., McGraw-Hill, Columbus, OH (2004).
13. J. Kolzer, E. Oesterschulze and G. Deboy, *Microelectronic Engineering*, **31**, 251 (1996).
14. C. C. Lee and J. Park, *IEEE Photonics Tech. Lett.*, **16**(7), 1706 (2004).
15. Y. Gu and N. Narendran, *Proc. of SPIE*, **5187**, 107 (2004).
16. Agilent Technologies, *Application Brief*, **A05** (1999).